Role of Non-Metallic Atom in Enhancing Catalytic Activity of Nickel-Based Compounds for Hydrogen Evolution Reaction

*Xingqun Zheng#[a], Lishan Peng#[a], Li Li *[a], Na Yang[a], Yanjun Yang[a], Jing Li[a], Jianchuan Wang[a,b] and Zidong Wei*[a]*

[a]The State Key Laboratory of Power Transmission Equipment & System Security and New Technology, Chongqing Key Laboratory of Chemical Process for Clean Energy and Resource Utilization, School of Chemistry and Chemical Engineering, Chongqing University, Shazhengjie 174, Chongqing 400044. [b]Key Laboratory of Fuel Cell Technology of Hubei Province, Wuhan University of Technology, Wuhan 430070, P. R. China

*Email: liliracial@cqu.edu.cn ; zdwei@cqu.edu.cn .

1. Experimental details

Preparation of the Ni(OH)$_2$ precursors. All chemical reagents used in this experiment were of analytical grade and were used without any further purification. Prior to the loading of the precursor, the Ni foam (50 mm×10 mm×1 mm) was ultrasonically cleaned in a 3.0 M HCl solution for 15 min to remove the surface oxide layer, then rinsed with DI water and dried in air. Afterwards, 35.0 mL of pink aqueous solutions consisting of 40.0 mM $Ni(NO_3)_2$•$6H_2O$, 200.0 mM $(NH_2)_2CO$ and 200.0 mM NH_4F were transferred into a Teflon-lined stainless steel autoclave with the treated Ni foam, which was placed at a certain angle. The autoclave was sealed and subsequently heated to 120 °C for 6 h. When the hydrothermal reaction was over, the samples were washed with DI water and dried in an oven at 60 °C for 12 h.

Preparation of the Ni-Ni$_3$S$_2$. The Ni-based precursor was converted into $Ni(SOH)_x$ while maintained the morphology of the precursor using a simple hydrothermal treatment. A certain amount of Na_2S•$9H_2O$ was added into DI water (35.0 mL) to form a homogenous solution. Then, the Na_2S solution was transferred into the autoclave with the $Ni(OH)_2$ precursor and heated in an oven at 160°C for 6 h. After being cooled to room temperature naturally, the Ni foam was removed, washed with DI water and absolute ethanol several times each, and dried in an oven at 60 °C for 2 h. Finally, all the samples were reduced under a H_2/N_2 atmosphere at 400 °C for 1 hour to obtain the Ni with different S contents. The $Ni(OH)_2$ precursor treated with the Na_2S•$9H_2O$ with different concentration of 5.0 mM, 10.0 mM, 20.0 mM, 40.0 mM and 80.0 mM were marked as Ni-Ni_3S_2-1, Ni-Ni_3S_2-2, Ni-Ni_3S_2-3, Ni-Ni_3S_2-4, Ni-Ni_3S_2-5, respectively.

Preparation of the pure Ni$_3$S$_2$. The precursor of $Ni(OH)_2$ was immersed into a solution consisted of 0.1 g $Na_2S{\cdot}9H_2O$ and 35 mL N_2H_4 H_2O in a 40 mL Teflon-lined stainless steel autoclave. The autoclave was then sealed and maintained at 180 °C for 12 h. After being cooled to room temperature naturally, the Ni foam was removed, washed with DI water and absolute ethanol several times each, and dried in an oven at 60 °C for 2 h.

2. Structure and morphology characterization

The surface morphology and the microstructure of the catalysts were analyzed by X-ray diffraction (XRD-6000, Shimadzu), X-ray photoelectron spectroscopy (XPS, PHI 550 ESCA/SAM), field-emission scanning electron microscopy (FE-SEM, JSM-7800, Japan), respectively.

3. Electrochemical characterizations

Electrochemical measurements were performed in 1 M KOH alkaline electrolyte with a three-electrode cell system by a CHI660D electrochemical analyzer (CH Instruments, Inc., Shanghai). Sizable and shapeable electrodes can be prepared by simply tailoring the Ni foam, and the obtained Ni-Ni_3S_2 can be directly used as the working electrode (1 cm^2) without employing extra substrates (e.g., glassy-carbon electrode) or binders (e.g., Nafion). A carbon rod in parallel orientation to the working electrode was used as the counter electrode with a distance of 1.0 cm and an Hg/HgO electrode was used as the reference electrode. The electrolyte was degassed by bubbling N_2 for at least 30 minutes before the electrochemical measurements. Linear sweep voltammetry (LSV) was performed in N_2 saturated aqueous solution with a scan rate of 10 $mV\cdot s^{-1}$ in a range from 0.2 to -0.6 V.

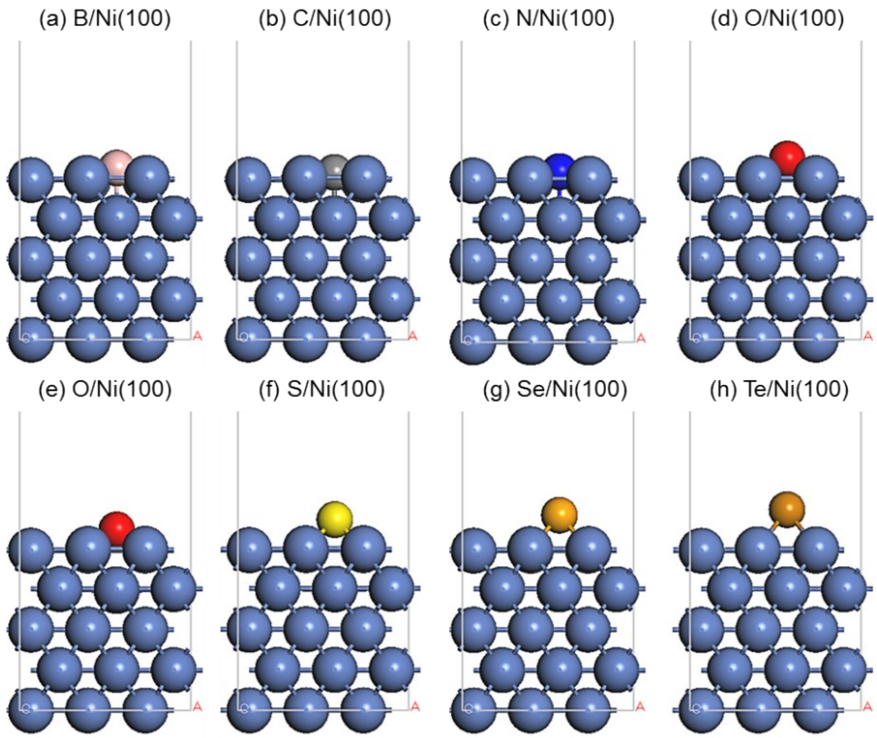

Fig. S1. The side view of the stable structure for each X/Ni(100) system. Color code: dusty blue, Ni atoms; other color, X atoms.

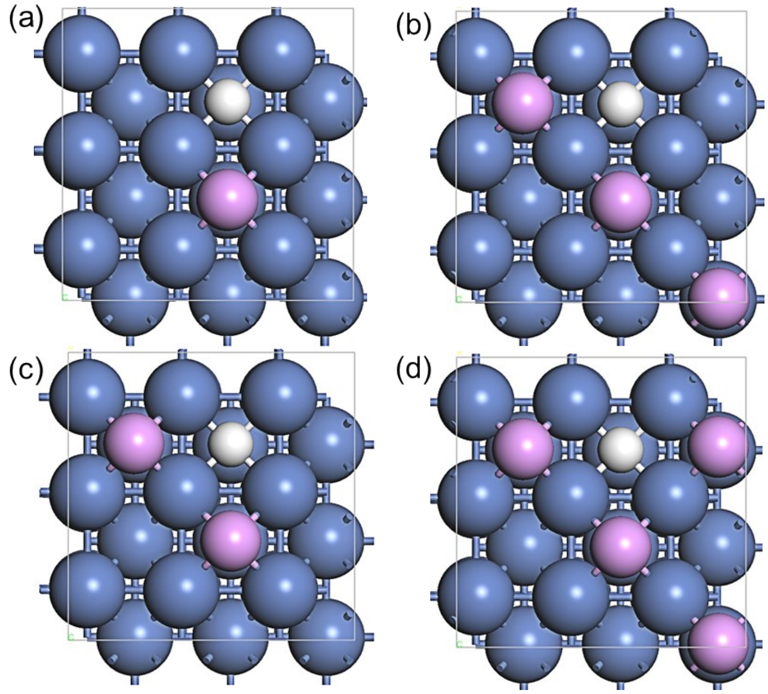

Fig. S2. The top view of unit cell structures of X_n/Ni(100) with H (white ball) adsorbed on them: (a)X/Ni(100); (b)X_2/Ni(100); (c)X_3/Ni(100); (d)X_4/Ni(100).

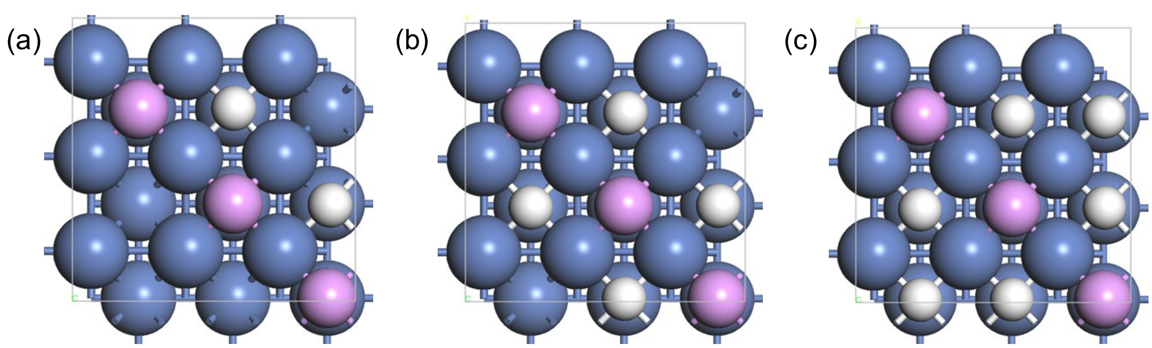

Fig. S3. The top view of unit cell structures of X_3/Ni(100) with different H coverage(θ_H): (a) θ_H=1/3; (b) θ_H=2/3; (c) θ_H=1.

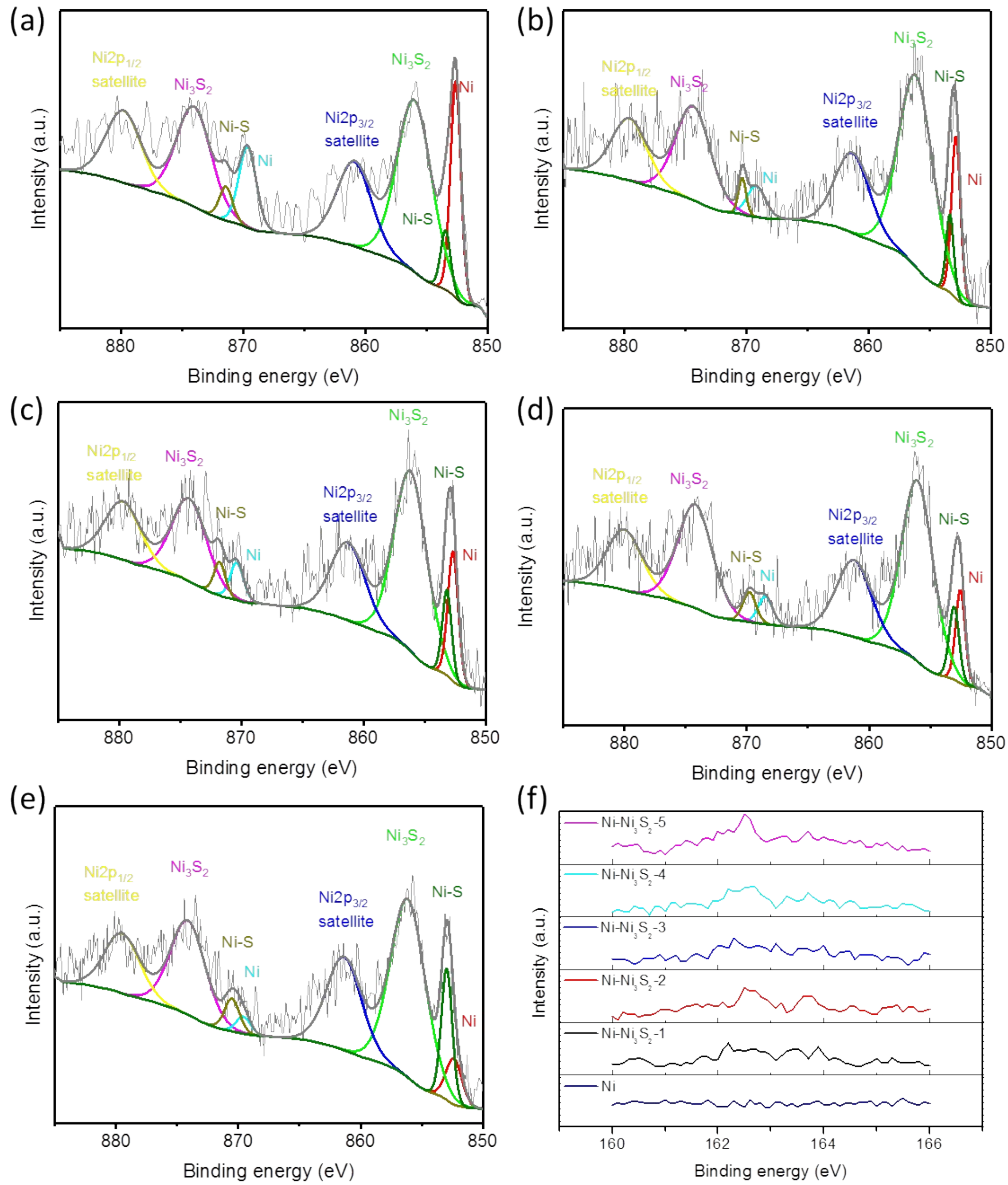

Fig. S4. Ni 2p core level X-ray photoelectron spectra (XPS): (a) Ni-Ni_3S_2-1; (b) Ni-Ni_3S_2-2; (c) Ni-Ni_3S_2-3; (d) Ni-Ni_3S_2-4; (e) Ni-Ni_3S_2-5; (f) S 2p core level XPS spectra of the Ni based catalysts

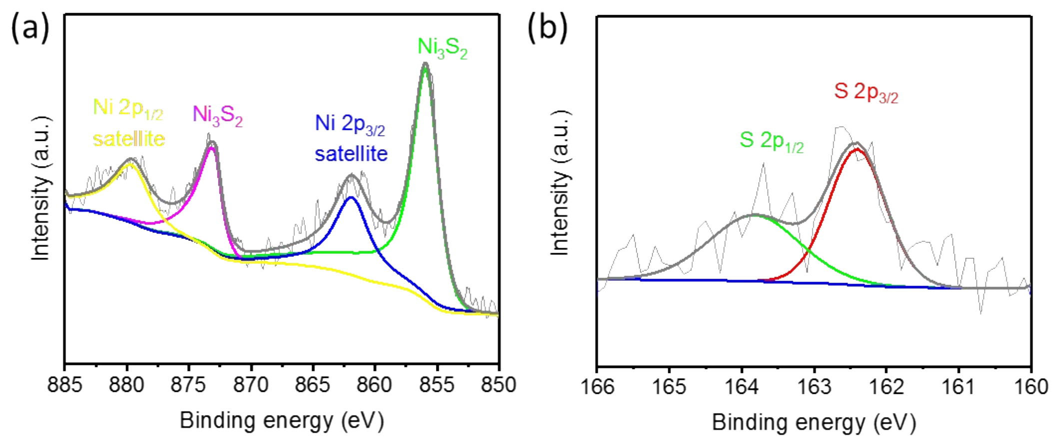

Fig. S5. Ni 2p and S 2p XPS of pure Ni_3S_2 catalyst.

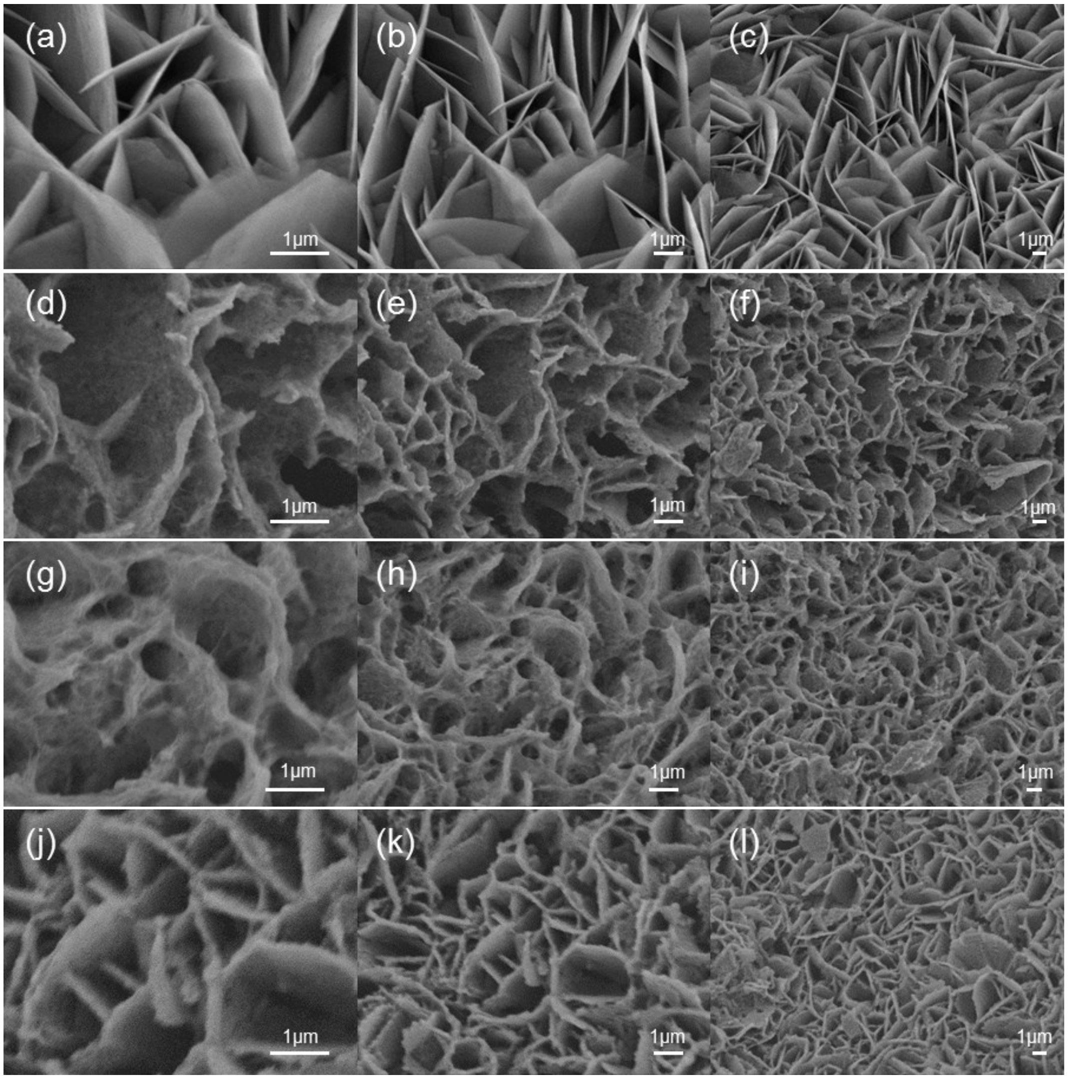

Fig. S6. The scanning electron microscopy (SEM) images with different magnifications: (a-c) Ni; (d-f) Ni-Ni_3S_2-1; (g-i) Ni-Ni_3S_2-3; (j-l) Ni-Ni_3S_2-5.

.

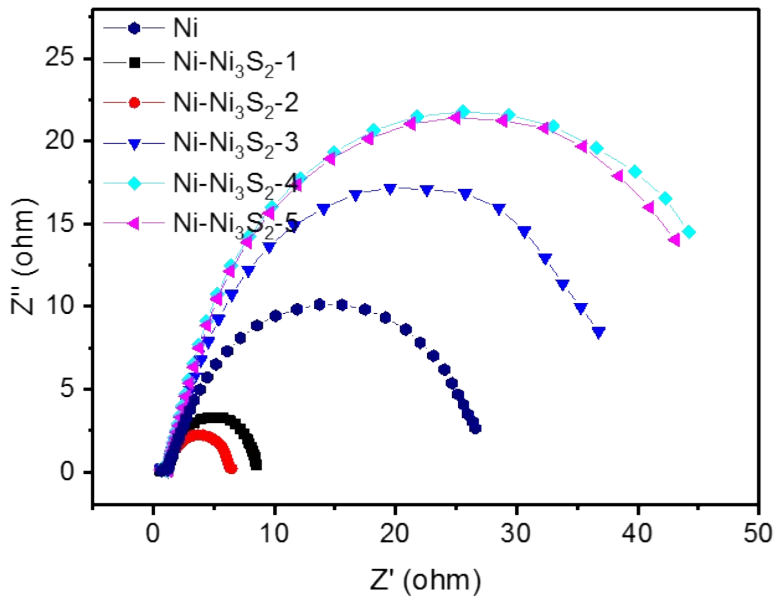

Fig. S7. Nyquist plots and the corresponding fitted curves of all samples.

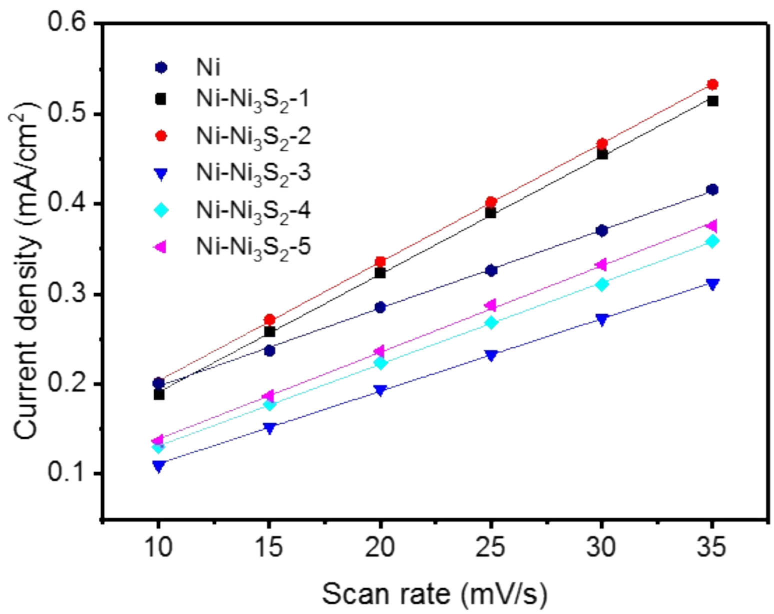

Fig. S8. Scan rate dependence of the current densities of all samples.

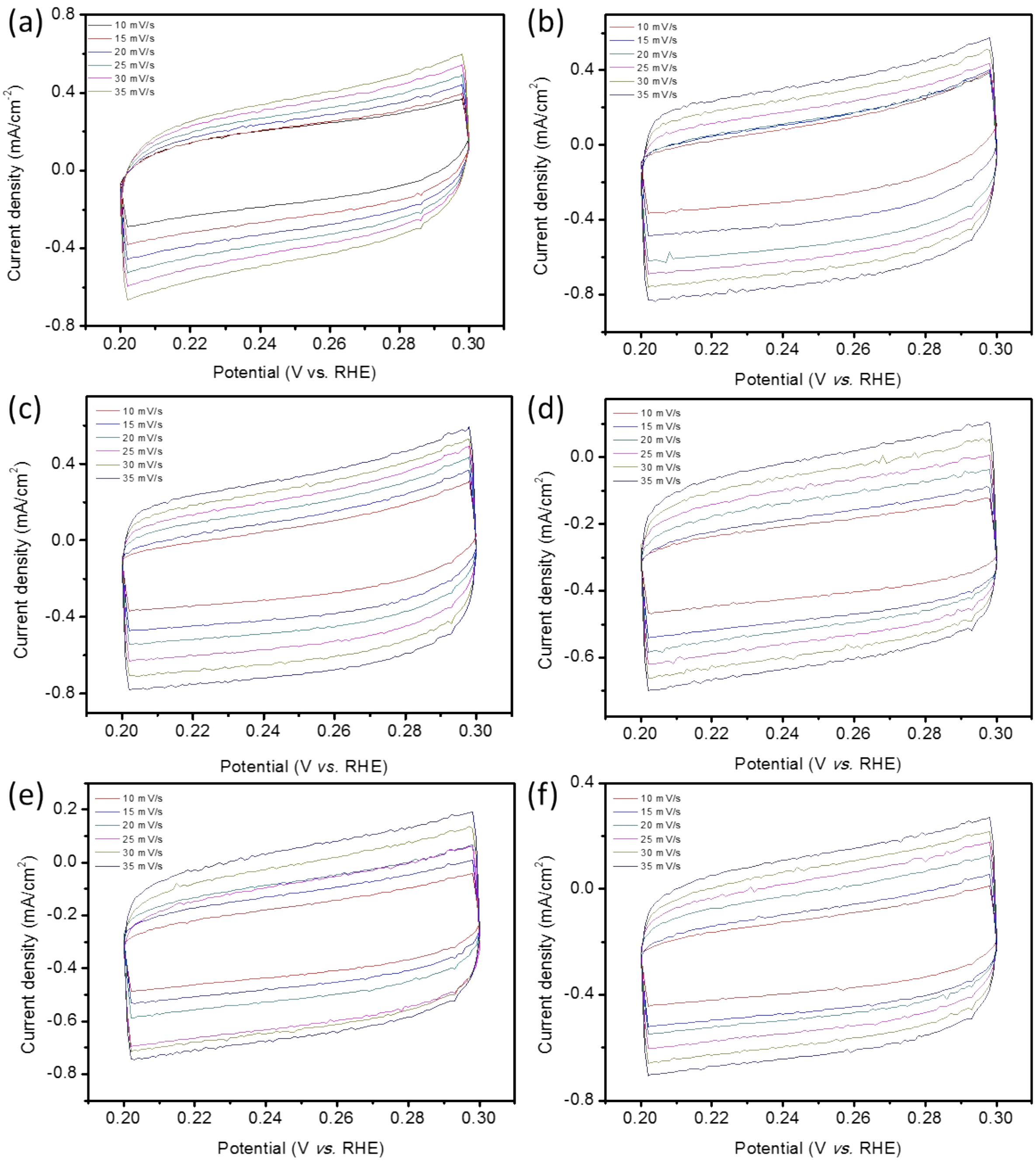

Fig. S9. Cyclic voltammograms of each sample: (a) Ni, (b) Ni-Ni_3S_2-1; (c) Ni-Ni_3S_2-2; (d) Ni-Ni_3S_2-3; (e) Ni-Ni_3S_2-4; (f) Ni-Ni_3S_2-5 in 0.20 – 0.30 V vs. RHE at scan rates from10 to 35 $mV \cdot s^{-1}$ in 1.0 M KOH

Table S1. Element electronegativity[1] (χ_X), atom radius[2] (R_X /Å), X-Ni bond length ($d_{X\text{-}Ni}$/Å) and interface Ni-Ni bond length ($d_{Ni\text{-}Ni}$/Å) of each X/Ni(100) system and the Bader charge of X(Q_x) and interface Ni (Q_{Ni}).

System	χ_{Ni} or χ_X	R_{Ni} or R_X/Å	Bond length/ Å		Bader charge/e	
			$d_{X\text{-}Ni}$	$d_{Ni\text{-}Ni}$	Q_X	Q_{Ni}
Ni(100)	1.91	1.35	-	2.492	-	-0.009
B/Ni(100)	2.04	0.85	1.906	2.628	-0.107	0.015
C/Ni(100)	2.55	0.70	1.837	2.579	-0.750	0.160
N/Ni(100)	3.04	0.65	1.833	2.555	-0.979	0.205
O/Ni(100)	3.44	0.60	1.947	2.489	-0.930	0.212
S/Ni(100)	2.58	1.00	2.184	2.536	-0.504	0.113
Se/Ni(100)	2.55	1.15	2.332	2.552	-0.323	0.058
Te/Ni(100)	2.10	1.40	2.503	2.567	-0.048	-0.010

Table S2. X binding energies (ΔE_X) and H adsorption energy (ΔE_H) (in eV), zero-point energies

ΔZPE (in eV), entropies multiplied by T (T = 298.15 K) (in eV), adsorption free energies ΔG_{H*} (in eV) of Ni(100) and all X/Ni(100) systems.

Systems	ΔE_X	ΔE_{H*}	ΔZPE	$T\Delta S$	ΔG_{H*}
Ni(100)	-	-0.490	-0.017	0.202	-0.305
B/Ni(100)	-7.115	-0.478	-0.023	0.202	-0.299
C/Ni(100)	-8.270	-0.476	-0.019	0.202	-0.293
N/Ni(100)	-6.130	-0.442	-0.016	0.202	-0.256
O/Ni(100)	-6.007	-0.402	-0.015	0.202	-0.215
S/Ni(100)	-6.014	-0.374	-0.016	0.202	-0.188
Se/Ni(100)	-5.349	-0.371	-0.017	0.202	-0.186
Te/Ni(100)	-4.906	-0.366	-0.019	0.202	-0.183
Pt(111)	-	-0.380	0.000	0.202	-0.178

Table S3. The ΔE_{H*}, ΔZPE (in eV), entropies multiplied by T (T = 298.15 K) (in eV), ΔG_{H*} (in eV) of X_n/Ni(100) (X=O, S, Se, Te) systems.

Number of X(n)	Systems	ΔE_{H*}	ΔZPE	$T\Delta S$	ΔG_{H*}
2	O_2/Ni(100)	-0.327	-0.007	-0.202	-0.132
	S_2/Ni(100)	-0.324	-0.008	-0.202	-0.130
	Se_2/Ni(100)	-0.335	-0.009	-0.202	-0.142
	Te_2/Ni(100)	-0.347	-0.011	-0.202	-0.156
3	O_3/Ni(100)	-0.305	0.001	-0.202	-0.102
	S_3/Ni(100)	-0.276	-0.001	-0.202	-0.075
	Se_3/Ni(100)	-0.284	-0.001	-0.202	-0.083
	Te_3/Ni(100)	-0.297	-0.002	-0.202	-0.097
4	O_4/Ni(100)	-0.036	0.015	-0.202	0.181
	S_4/Ni(100)	-0.036	0.017	-0.202	0.182
	Se_4/Ni(100)	-0.076	0.014	-0.202	0.140
	Te_4/Ni(100)	-0.127	0.011	-0.202	0.086

Table S4. The ΔE_{H*}, ΔZPE (in eV), entropies multiplied by T (T = 298.15 K) (in eV), ΔG_{H*} (in eV) of X_3/Ni(100) (X=O, S, Se, Te) with different θ_H (from 1/3 to 1).

θ_H	Systems	ΔE_{H*}	ΔZPE	$T\Delta S$	ΔG_{H*}
1/3	O_3Ni(100)	-0.307	0.004	-0.202	-0.101
	S_3Ni(100)	-0.273	0.001	-0.202	-0.070
	Se_3Ni(100)	-0.283	0.001	-0.202	-0.079
	Te_3Ni(100)	-0.296	-0.001	-0.202	-0.095
2/3	O_3Ni(100)	-0.279	0.005	-0.202	-0.071
	S_3Ni(100)	-0.250	0.006	-0.202	-0.041
	Se_3Ni(100)	-0.264	0.004	-0.202	-0.058
	Te_3Ni(100)	-0.282	0.002	-0.202	-0.078
1	O_3Ni(100)	-0.259	0.009	-0.202	-0.048
	S_3Ni(100)	-0.229	0.010	-0.202	-0.016
	Se_3Ni(100)	-0.249	0.008	-0.202	-0.039
	Te_3Ni(100)	-0.269	0.006	-0.202	-0.061

Table S5. Atomic ratio of Ni, S coming from XPS analysis.

Samples	***Area of Ni 2p3/2***	***Area of Ni-S 2p3/2***	***S coverage***
Ni-Ni_3S_2-1	1253.58	327.06	20.67%
Ni-Ni_3S_2-2	670.41	272.95	28.93%
Ni-Ni_3S_2-3	660.26	390.58	37.17%
Ni-Ni_3S_2-4	435.05	358.86	45.20%
Ni-Ni_3S_2-5	359.25	710.93	66.43%

Table S6. The surface S:Ni atomic ratio, overpotential@10mA/cm^2 (mV), Tafel slope(mV dec^{-1}), C_{dl} (mF·cm^{-2}) and relative surface area of Ni and all $Ni-Ni_3S_2$ catalysts.

Catalysts	S:Ni (%)	Overpotential @10mA·cm^{-2} (mV)	Tafel slope (mV·dec^{-1})	C_{dl} (mF·cm^{-2})	Relative surface area	Ref
Ni	-	225	126	8.67	0.66	In this work
$Ni-Ni_3S_2$-1	20.67	129	126	13.08	0.99	In this work
$Ni-Ni_3S_2$-2	**28.93**	**114**	**122**	**13.18**	**1**	In this work
$Ni-Ni_3S_2$-3	37.17	154	157	7.34	0.56	In this work
$Ni-Ni_3S_2$-4	45.20	180	154	9.06	0.69	In this work
$Ni-Ni_3S_2$-5	66.43	181	159	9.61	0.93	In this work
$Ni_{2.3\%}CoS_2$/CC	--	136	106	--	--	[3]
NiCoS/CC NSs	--	140	96	--	--	[4]
NiS/Ni Foam	--	150	83	--	--	[5]
$NiCo_2S_4$ NA/CC	--	~190	141	--	--	[6]
Ni_3S_2@Ni	--	195	107	--	--	[7]
Ni_3S_2-Ni	--	270	141	--	--	[7]
Ni_xS_y/NiF	--	230	87	--	--	[8]
$Co_9S_8-Ni_xS_y$/NiF	--	163	88	--	--	[8]

REFERENCE

1 L. Pauling, *The Nature of the Chemical Bond,* 3rd ed, Cornell University Press: Ithaca, New York, 1960

2 J. C. Slater, Atomic Radii in Crystals. *J. Chem. Phys.*, 1964, **41**, 3199-3204.

3 W. Fang, D. Liu, Q. Lu, X. Sun and A. M. Asiri, *Electrochem. Commun*., 2016, **63**, 60-64.

4 C. Tang, Z. Pu, Q. Liu, A. M. Asiri, Y. Luo and X. Sun, *Int. J. Hydrogen Energy*, 2015, **40**, 4727-4732.

5 W. Zhu, X. Yue, W. Zhang, S. Yu, Y. Zhang, J. Wang and J. Wang, *Chem. Commun.*, 2016, **52**, 1486-1489.

6 D. Liu, Q. Lu, Y. Luo, X. Sun and A. M. Asiri, *Nanoscale*, 2015, **7**, 15122-15126.

7 C. Ouyang, X. Wang, C. Wang, X. Zhang, J. Wu, Z. Ma, S. Dou and S. Wang, *Electrochim. Acta*, 2015, **174**, 297-301.

8 D. Ansovini, C. J. J. Lee, C. S. Chua, J. Ong, H. R. Tan, W.Webb, R. Raja and Y.-F. Lim, *J. Mater. Chem. A*, 2016, **4**, 9744-9749.